Artificial Intelligence In Medicine 137 (2023) 102496

Contents lists available at ScienceDirect

Artificial Intelligence In Medicine

journal homepage: www.elsevier.com/locate/artmed

Application of deep learning algorithms in automatic sonographic localization and segmentation of the median nerve: A systematic review and meta-analysis

Jia-Chi Wang [a,b], Yi-Chung Shu [c], Che-Yu Lin [c], Wei-Ting Wu [d,e], Lan-Rong Chen [d], Yu-Cheng Lo [c], Hsiao-Chi Chiu [c], Levent Özçakar [f], Ke-Vin Chang [d,e,g,*]

[a] *Department of Physical Medicine and Rehabilitation, Taipei Veterans General Hospital, Taipei, Taiwan*
[b] *School of Medicine, National Yang Ming Chiao Tung University, Taipei, Taiwan*
[c] *Institute of Applied Mechanics, College of Engineering, National Taiwan University, Taipei, Taiwan*
[d] *Department of Physical Medicine and Rehabilitation and Community and Geriatric Research Center, National Taiwan University Hospital, Bei-Hu Branch, Taipei, Taiwan*
[e] *Department of Physical Medicine and Rehabilitation, National Taiwan University College of Medicine, Taipei, Taiwan*
[f] *Department of Physical and Rehabilitation Medicine, Hacettepe University Medical School, Ankara, Turkey*
[g] *Center for Regional Anesthesia and Pain Medicine, Wang-Fang Hospital, Taipei Medical University, Taipei, Taiwan*

ARTICLE INFO

Keywords:
Artificial intelligence
Convolutional neural network
Ultrasonography
Carpal tunnel
Neuropathy

ABSTRACT

Objective: High-resolution ultrasound is an emerging tool for diagnosing carpal tunnel syndrome caused by the compression of the median nerve at the wrist. This systematic review and meta-analysis aimed to explore and summarize the performance of deep learning algorithms in the automatic sonographic assessment of the median nerve at the carpal tunnel level.

Methods: PubMed, Medline, Embase, and Web of Science were searched from the earliest records to May 2022 for studies investigating the utility of deep neural networks in the evaluation of the median nerve in carpal tunnel syndrome. The quality of the included studies was evaluated using the Quality Assessment Tool for Diagnostic Accuracy Studies. The outcome variables included precision, recall, accuracy, F-score, and Dice coefficient.

Results: In total, seven articles were included, comprising 373 participants. The deep learning and related algorithms comprised U-Net, phase-based probabilistic active contour, MaskTrack, ConvLSTM, DeepNerve, DeepSL, ResNet, Feature Pyramid Network, DeepLab, Mask R-CNN, region proposal network, and ROI Align. The pooled values of precision and recall were 0.917 (95 % confidence interval [CI], 0.873–0.961) and 0.940 (95 % CI, 0.892–0.988), respectively. The pooled accuracy and Dice coefficient were 0.924 (95 % CI, 0.840–1.008) and 0.898 (95 % CI, 0.872–0.923), respectively, whereas the summarized F-score was 0.904 (95 % CI, 0.871–0.937).

Conclusion: The deep learning algorithm enables automated localization and segmentation of the median nerve at the carpal tunnel level in ultrasound imaging with acceptable accuracy and precision. Future research is expected to validate the performance of deep learning algorithms in detecting and segmenting the median nerve along its entire length as well as across datasets obtained from various ultrasound manufacturers.

1. Introduction

Median nerve compression in the wrist region, i.e., carpal tunnel syndrome (CTS), is the most prevalent entrapment neuropathy [1]. Its diagnosis is traditionally established based on the electrophysiological findings such as slowed nerve conduction velocity, delayed distal motor latency, and abnormal thenar muscle electromyography [2]. Recently, high-resolution ultrasound imaging has been considered an alternative tool for diagnosing CTS owing to its explicit depiction of neural fascicles and surrounding connective tissues. The sonographic criteria for CTS diagnosis include increased cross-sectional area of the nerve [3], flattened nerve configuration [4], and increased nerve stiffness [5] and

Abbreviations: CTS, carpal tunnel syndrome; CNN, convolutional neural network; IOU, intersection over union.

* Corresponding author at: Department of Physical Medicine and Rehabilitation, National Taiwan University Hospital, Bei-Hu Branch, Taipei, Taiwan.
E-mail address: kvchang011@gmail.com (K.-V. Chang).

https://doi.org/10.1016/j.artmed.2023.102496
Received 20 May 2022; Received in revised form 13 November 2022; Accepted 18 January 2023
Available online 21 January 2023

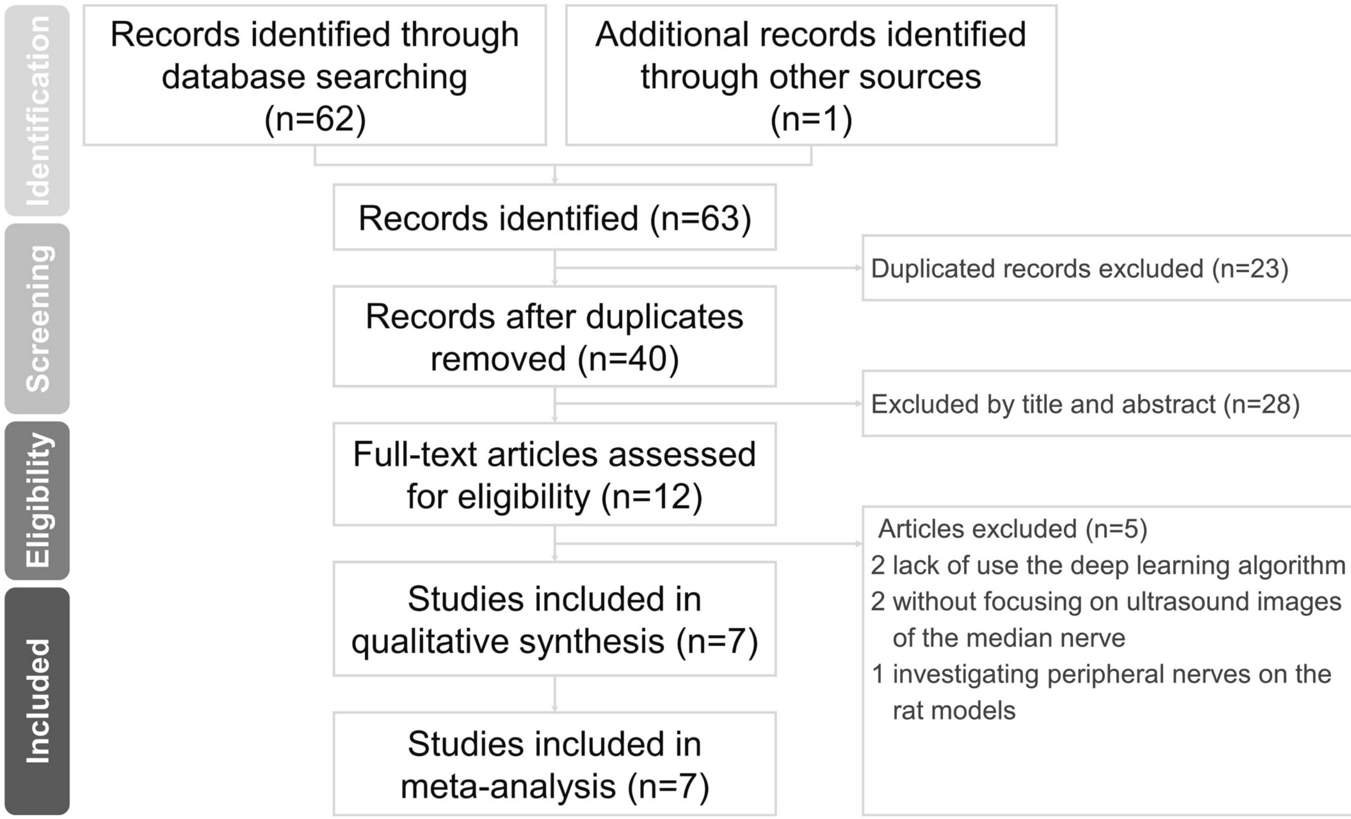

Fig. 1. Flow diagram of the literature search.

Table 1
Summary of the included studies.

Author/year	Participant number	Ultrasound machine/setting	Data set	Focused task	Deep learning (related) algorithm	Ground truth definer	Performance metric
Hafiane et al. (2017)	10	Unknown manufacturer with linear transducer of 5–12 MHz	10 videos with 500 frames per video	Localization and segmentation	CNN and phase based probabilistic active contour	Anesthesiology specialist	Precision, recall, F-score and disc coefficient
Horng et al. (2020)	6	Siemens ACUSON S2000 ultrasound system with an 18L6 HD transducer	Not mentioned	Localization and segmentation	U-Net, MaskTrack, ConvLSTM, and DeepNerve	Not mentioned	Precision, recall, F-score, accuracy and disc coefficient
Wang et al. (2020)	50	Not mentioned	180 continuous imaging slices for each hand	Localization	DeepSL and Resnet	Expert of sonography	Accuracy
Cosmo et al. (2020)	53	Esaote MyLab Class C with a 6–18 MHz linear transducer	Not mentioned	Localization and segmentation	Resnet, Feature Pyramid Network and Mask R-CNN	Not mentioned	Precision and disc coefficient
Festen et al. (2021)	99	Philips iE33 with a L15-7io linear transducer	A total of 5560 frames from 505 videos	Segmentation	U-Net	Not mentioned	Disc coefficient
Wu et al. (2021)	52	Canon Aplio 500 with a line transducer of 13–18 MHz	15,215 frames for training and 3410 frames for testing	Segmentation	U-Net, DeepLab, Feature Pyramid Network and Mask R-CNN	Physiatrist	Intersection over union
Smerilli et al. (2022)	103	Esaote MyLab Class C with a linear 6–18 MHz probe	157 images for training, 40 images for validation, and 49 images for testing	Localization and segmentation	ResNet, Feature Pyramid Network, region proposal network, ROI Align and Mask R-CNN	Rheumatologist	Precision, recall and disc coefficient

CNN, convolutional neural network.

intra-neural vascularity [6]. Furthermore, ultrasound allows dynamic examination, which can be used to assess the median nerve mobility along with CTS severity [7].

Among all the sonographic diagnostic criteria of CTS, the cross-sectional area of the nerve appears to be the most validated parameter, which can be applied in the general population [3] and in patients with pre-existing diabetes mellitus [8]. However, correct identification of the median nerve may be challenging for inexperienced examiners, not to mention the standardized assessment of its size. Moreover, it would be labor-intensive and time-consuming if the investigators intend to conduct serial manual measurements using dynamic images. Recently, artificial intelligence has been developed to assist nerve identification using ultrasound images. In 2016, Hadjerci et al. [9] constructed a computer-aided system for the automatic detection and segmentation of the median nerve. Nevertheless, the preliminary framework required multiple stages, such as the implementation of

Table 2
Summary of Quality Assessment as regards the included studies.

	Risk of Bias				Application Concern		
Study name	Patient Selection	Index Test	Reference Standard	Flow Timing	Patient Selection	Index Test	Reference Standard
Hafiane et al. 2017	?	✓	✓	✓	✓	✓	✓
Horng et al. 2020	?	✓	✗	✓	✓	✓	✓
Wang et al. 2020	?	✓	✓	✓	✓	✓	✓
Cosmo et al. 2020	?	✓	✗	✓	✓	✓	✓
Festen et al. 2021	✓	✓	✗	✓	✓	✓	✓
Wu et al. 2021	✓	✓	✓	✓	✓	✓	✓
Smerilli et al. 2022	?	✓	✓	✓	✓	✓	✓

Green; low risk of bias, Red; high risk of bias, Yellow; unclear risk of bias.

various despeckling filters, extraction of different features, and selection of the best feature subset, which prevented it from being an end-to-end process. Deep learning, inspired by the structure of the human brain, enables the automatic selection of features from the given data and is being increasingly used in biomedical analysis [10].

Among all the deep learning algorithms, the convolutional neural network (CNN) is one of the most powerful frameworks for investigating visual imagery [11]. Recent studies have applied CNN for identifying neural vascular structures over the axillary [12] and femoral regions [13]. Owing to the clinical importance of CTS, several studies have investigated the feasibility of deep learning algorithms in the sonographic evaluation of the median nerve in the wrist region. Therefore, this systematic review and meta-analysis aimed to explore and summarize the performance of deep learning in the automatic localization and segmentation of the median nerve at the carpal tunnel level.

2. Methods

2.1. Protocol registration

This meta-analysis was conducted in compliance with the guidelines of the Preferred Reporting Items for Systematic Reviews and Meta-Analyses (PRISMA) program, with the protocol registered on Inplasy.com (INPLASY202250074).

2.2. Literature search

The following electronic databases were searched from their inception to May 2022: PubMed, Medline, Embase, and Web of Science. Studies investigating the utility of deep neural networks in the evaluation of the median nerve at the carpal tunnel level were targeted. Key terms used for the literature search included "median nerve," "carpal tunnel syndrome," "ultrasonography," "sonography," "ultrasound," "artificial intelligence," "deep learning," "machine learning," and "convolutional neural network." The following algorithm was used: ("median nerve" or "carpal tunnel syndrome") and ("ultrasonography" or "ultrasound" or "sonography") and ("artificial intelligence" or "deep learning" or "machine learning" or "convolutional neural network"). No language restrictions were imposed during the search process. In addition, relevant narratives and systematic reviews were inspected for potentially eligible studies.

2.3. Inclusion and exclusion criteria

The population, intervention, comparison, and outcome setting (commonly called PICO) of the current systematic review and meta-analysis comprised: (1) P: human; (2) I: evaluation of the cross-sectional ultrasound images of the median nerve using deep learning; (3) C: manually labelled region as the ground truth; and (4) O: performance metrics, such as precision, recall, accuracy, F-score, and Dice coefficient.

The inclusion criteria were as follows: (1) observational studies recruiting adult participants aged $\geq$20 years; (2) use of ultrasound imaging to assess the median nerve; and (3) application of CNN for the localization and segmentation of the median nerve.

The exclusion criteria were as follows: (1) studies using animals or computer simulation only; (2) evaluation of the median nerve using modalities other than sonography; (3) focusing on the peripheral nerve outside the carpal tunnel; and (4) lack of application of any deep learning algorithm.

2.4. Quality Assessment

The quality of the included studies was evaluated using the second version of the Quality Assessment Tool for Diagnostic Accuracy Studies (QUADAS-2) [14]. This tool comprises four major domains of patient selection, index test, reference standard, and flow of timing regarding the index test and reference standard. For the patient selection domain, the authors focused on whether CTS was diagnosed using clearly defined criteria. For the index test domain, the authors evaluated whether the deep learning algorithm for appraising the median nerve was explicitly described. For the reference standard domain, the authors checked whether the ground truth (manually labelled nerve regions) was determined by experienced specialists. Finally, as training of the deep learning model was conducted after the completion of manual marking, clarity of the research flow was confirmed for all the included studies.

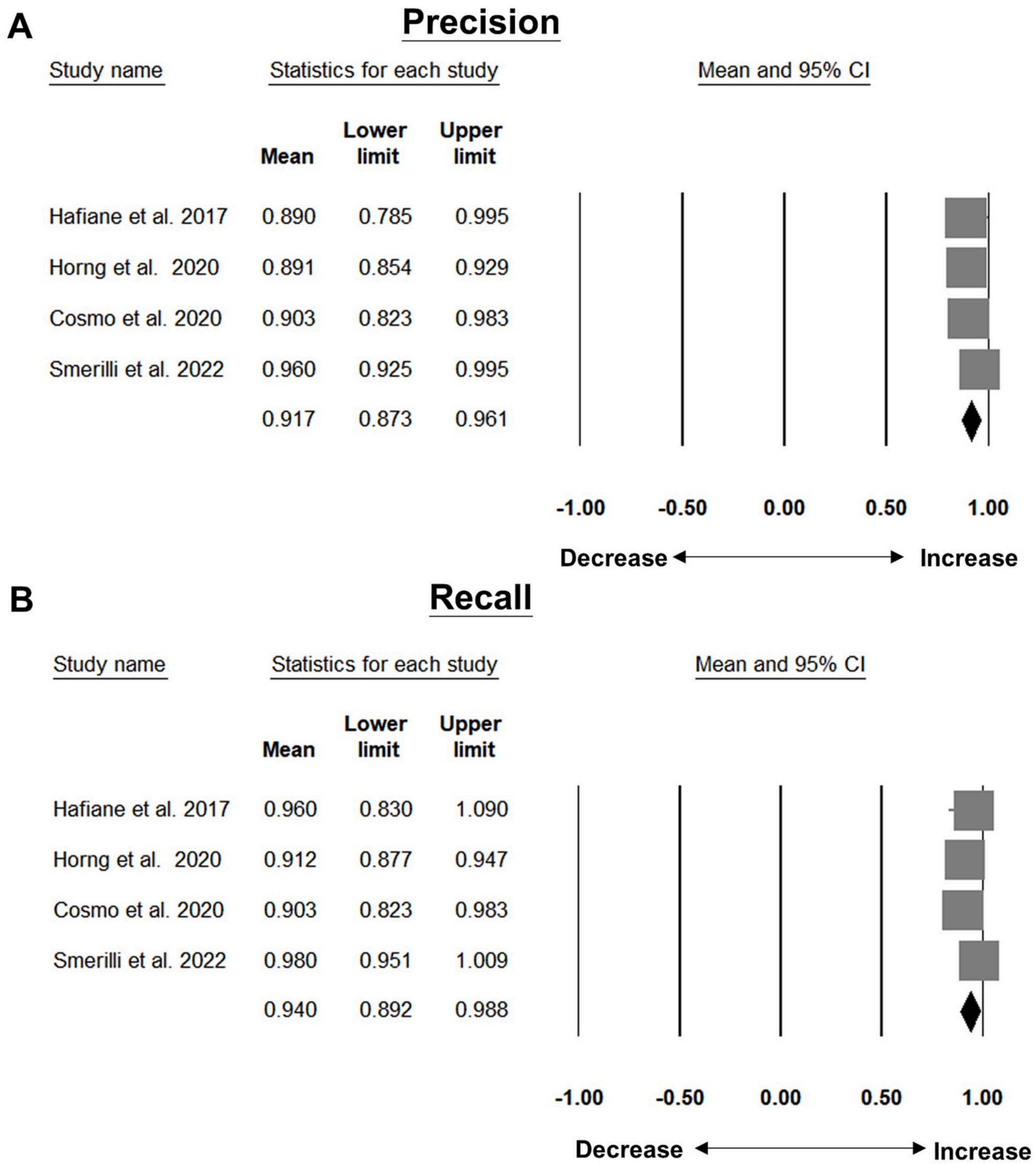

Fig. 2. Forest plot of the summarized precision (A) and recall (B) of the included studies.

2.5. Data extraction and outcome evaluation

The data extraction was conducted by two independent authors, and the following information was retrieved: authors, year, study design, participant characteristics, ultrasound machine, details of the dataset, models or architecture of artificial neural networks, and related performance metrics. The outcome variables comprised precision, recall, accuracy, F-score, Dice similarity coefficient, and intersection over union (IOU) [15].

$$\text{Precision} = \frac{TP}{TP + FP} \tag{1}$$

$$\text{Recall} = \frac{TP}{TP + FN} \tag{2}$$

$$\text{Accuracy} = \frac{TP + TN}{TP + TN + FP + FN} \tag{3}$$

$$F - \text{score} = \frac{2 \times \text{Precision} \times \text{Recall}}{\text{Precision} + \text{Recall}} \tag{4}$$

$$\text{Dice similarity coefficient} = \sum_{i=1}^{n} \frac{2|GT_i \cap SR_i|}{|GT_i| + |SR_i|} \tag{5}$$

Here, TP, TN, FP, and FN denote true positive, true negative, false positive, and false negative, respectively. GT_i and SR_i indicate the manually labelled region (ground truth) and the result derived from the deep learning algorithm in the *i*th frame, respectively. Finally, IOU denotes the overlapped region between the anticipated segmentation and the manually defined area divided by the region of union of both the parts.

2.6. Statistical analysis

A random effects model was used to pool the retrieved data considering the variations in participants' demographics [16]. The continuous variables are presented as means and standard errors. Data from the model proposed by the authors for meta-analysis were retrieved if several deep-learning algorithms were applied in the same study. The level of heterogeneity was assessed using I^2 and Cochran's Q statistics. An I^2 value > 50 % indicated moderate to high heterogeneity [17]. Publication bias was evaluated by the distribution of each effect size in

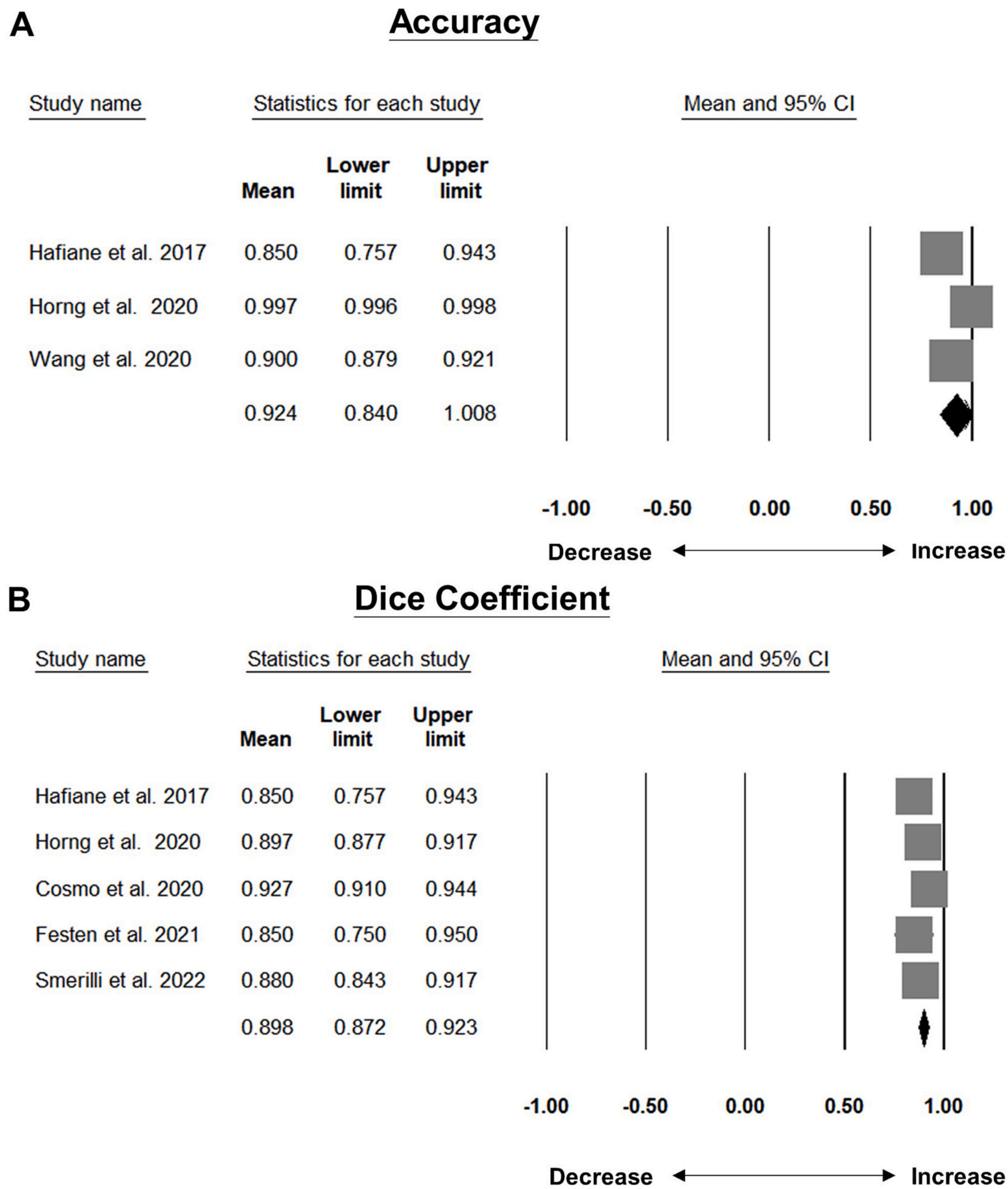

Fig. 3. Forest plot of the summarized accuracy (A) and Dice coefficient (B) of the included studies.

the funnel plot and Egger's test [18]. All analyses were conducted using Comprehensive Meta-Analysis software, version 3 (Biostat, Englewood, NJ, USA); *p*-values < 0.05 were considered statistically significant.

3. Results

3.1. Study selection

The flow of the literature search is presented in Fig. 1. The full texts of 63 articles were retrieved for eligibility evaluation after removing duplicated and irrelevant articles by surveying their titles and abstracts. We further excluded two papers due to lack of application of deep learning algorithms [19,20], two for not focusing on the ultrasound images of the median nerve [13,21], and one for investigating peripheral nerves in rat models [22]. Our systematic review and meta-analysis included seven articles [23–29] comprising 373 participants.

3.2. Study characteristics

All the included studies employed a cross-sectional design. The number of recruited participants ranged from 6 to 103 (Table 1). The ultrasound systems used for imaging were ACUSON S2000 (Siemen Medical Solutions, Mountain View, CA, USA), MyLab Class C (Esaote Spa, Genoa, Italy), Philips iE33 (Philips Ultrasound, Inc., Bothell, WA, USA), and Aplio 500 (Canon Medical Systems Europe B.V., The Netherlands). The deep learning and related algorithms used comprised U-Net [24,27,28], phase-based probabilistic active contour [23], MaskTrack [24], ConvLSTM [24], DeepNerve [24], DeepSL [25], ResNet [25,26], Feature Pyramid Network (FPN) [26,28,29], DeepLab [28], Mask R-CNN [26,28,29], region proposal network [29], and ROI Align [29]. Regarding the target tasks for processing the nerve imaging, one study [25] focused on localization, two studies [27,28] focused on segmentation and four studies [23,24,26,29] focused on both localization and segmentation. The reported performance metrics included precision, recall, accuracy, F-score, Dice coefficient, and IOU. The

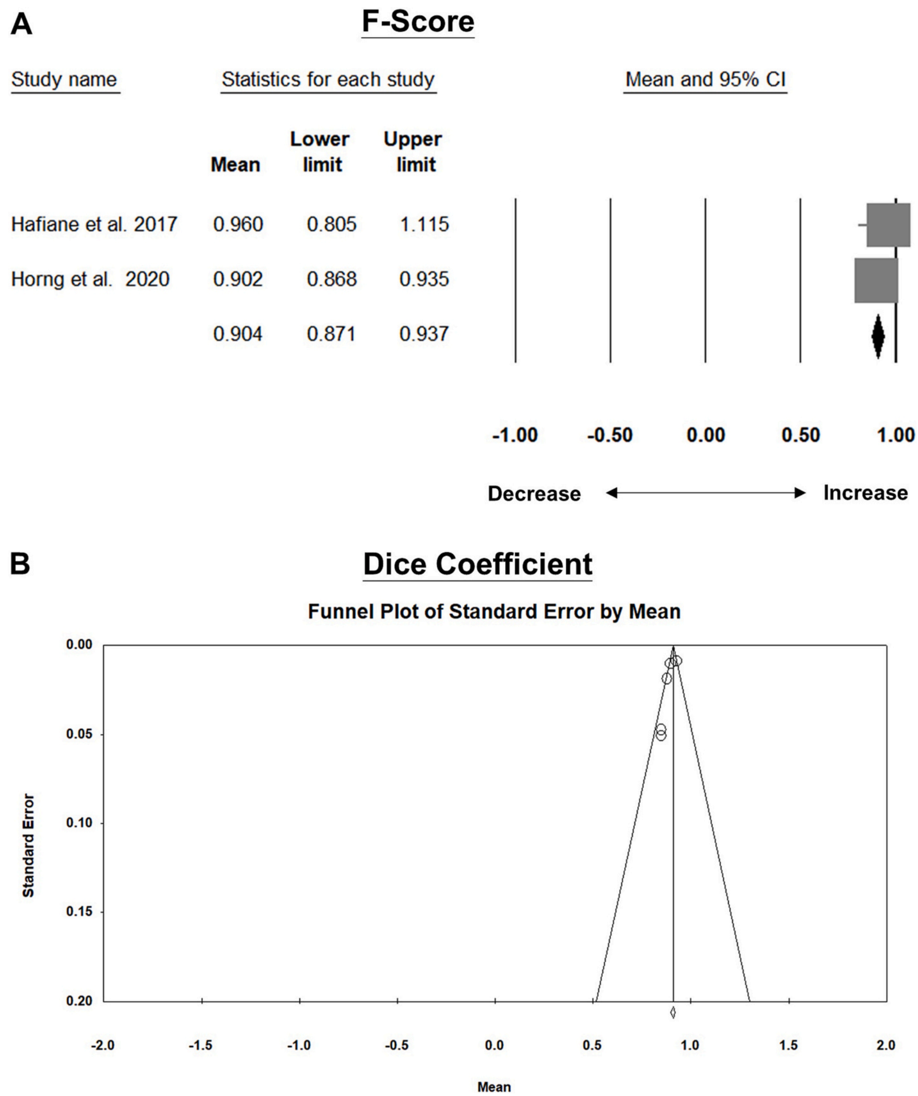

Fig. 4. Forest plot of the summarized F-score (A) and funnel plot of the Dice coefficient (B) of the included studies.

application of CNN for measuring circularity, cross-sectional area, perimeter, and vertical/horizontal displacement of the median nerve during finger motions was specifically reported in three studies [24,25,28]. Only one study addressed the influence of the anatomic variations on the performance metrics [29].

3.3. Methodological quality of included studies

The appraisal of the methodological quality of the included studies is presented in Table 2. Among the seven items of the QUADAS-2 tool, the most commonly failed item was the applicability concern regarding patient selection. The main reason for this was that only two studies [27,28] included patients diagnosed with CTS using clearly defined criteria, which might limit the clinical applicability of our meta-analysis. The second most commonly failed item was the risk of bias for the reference standard, because majority of the enrolled studies did not clarify the qualifications of the experts labelling the location and contour of the median nerve.

3.4. Performance metrics for localization and segmentation of the median nerve

The pooled values of precision and recall from four studies [23,24,26,29] were 0.917 (95 % confidence interval [CI], 0.873–0.961; $I^2 = 61.08$ %; $p = 0.052$) and 0.940 (95 % CI, 0.892–0.988; $I^2 = 70.03$ %; $p = 0.001$), respectively (Fig. 2). The pooled value of accuracy from three studies [23–25] was 0.924 (95 % CI, 0.840–1.008; $I^2 = 97.83$ %; $p < 0.001$). The pooled Dice coefficient from five studies [23,24,26,27,29] was 0.898 (95 % CI, 0.872–0.923; $I^2 = 63.14$ %; $p < 0.028$) (Fig. 3). The summarized F-score from two studies [23,24] was 0.904 (95 % CI, 0.871–0.937; $I^2 < 0.01$ %; $p = 0.049$) (Fig. 4). Only one study [28] reported IOU, with the average value between 0.7873 and 0.8216 across different deep learning algorithms.

3.5. Publication bias

The analysis of publication bias was performed only for the Dice coefficient, because the number of available studies for the other outcome parameters was largely insufficient ($n < 5$) (Fig. 4). The p-value of the Egger's test was 0.153, indicating no significant publication bias.

4. Discussion

This meta-analysis is possibly the first to explore and show that deep learning algorithms have acceptable accuracy and precision in the localization and segmentation of the median nerve near the carpal

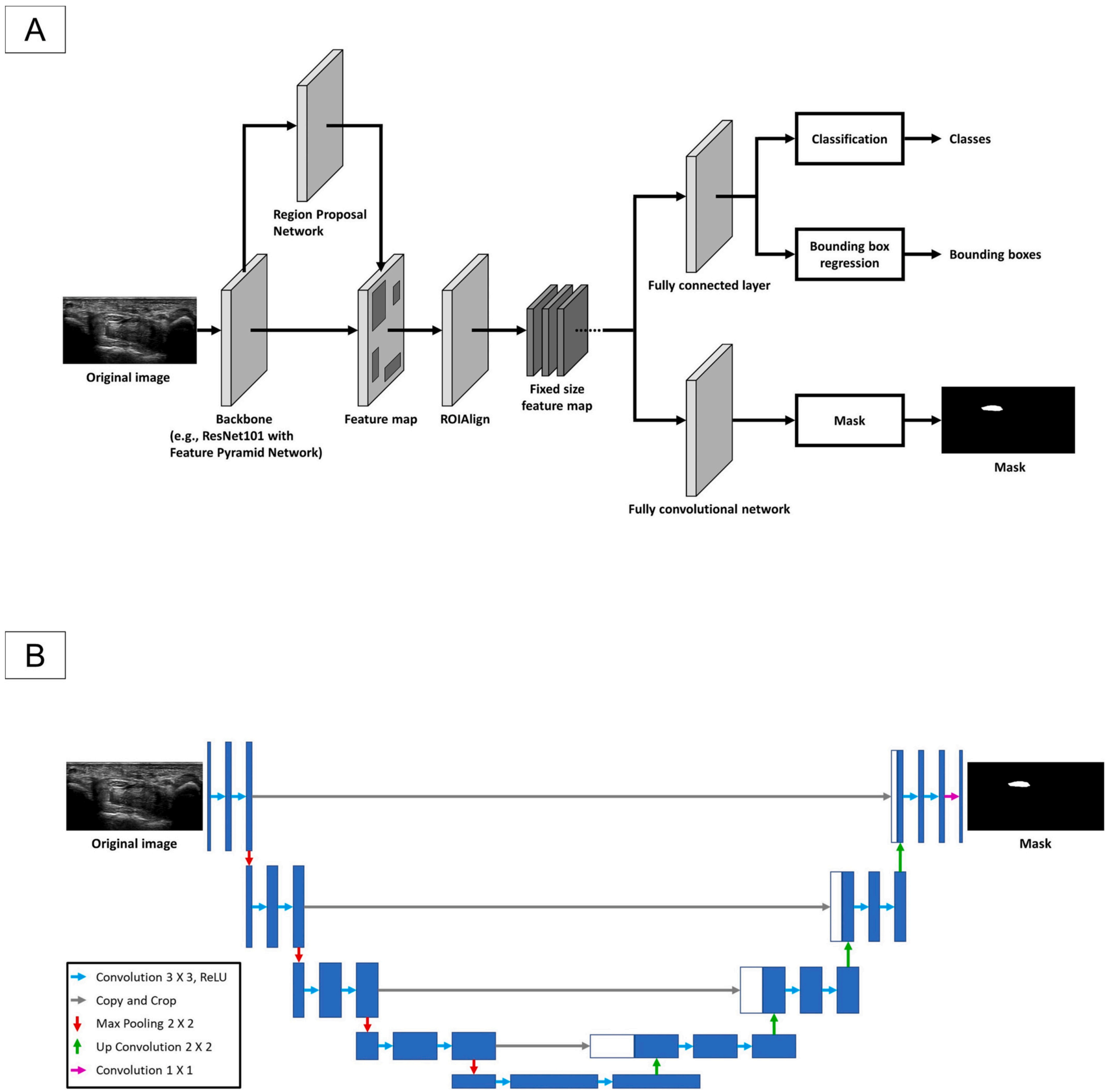

Fig. 5. Illustration of Mask R-CNN (A) and U-net (B) for segmentation of the median nerve.

tunnel. Our investigation revealed the potential of deep learning algorithms in motion metrics, i.e., the assessment of the median nerve during finger flexion and extension. The impact of anatomical variations on the detection of the median nerve was also investigated in this review.

Different strategies have been applied for localization, which is the process of identifying the region of interest (ROI) that contains the median nerve. Hafiane et al. [23] took the advantage of the spatial and temporal consistency of the median nerve while mobilizing the transducer over the wrist. A sliding window was applied to the target frames, and the CNN helped to classify whether the ROI included the median nerve. An area overlapped spatially by several ROIs with high probability of including the nerve would be the candidate. Furthermore, if the candidate zone was consistently recognized in different frames, the area where the median nerve was located was determined by employing the rule of temporal consistency. Similarly, Wang et al. [25] developed a learning model by comparing the similarity between the target ROI and the candidate regions using two convolutions, two maximal pooling, and one difference layer. ResNet [30] was employed for similarity differentiation. In our meta-analysis, precision, recall, accuracy, and F-score were used to evaluate the performance metrics for the localization of the median nerve. All the pooled values of the aforementioned parameters were >0.9. Our results demonstrate the capability of deep learning algorithms in correctly identifying the location of the median nerves on the given ultrasound images.

Clinically, segmentation of the nerve (demarcating the nerve boundary) is more important than localization. Segmentation of the median nerve is crucial for the measurement of its cross-sectional area and determination of its shape, which have been widely used for CTS

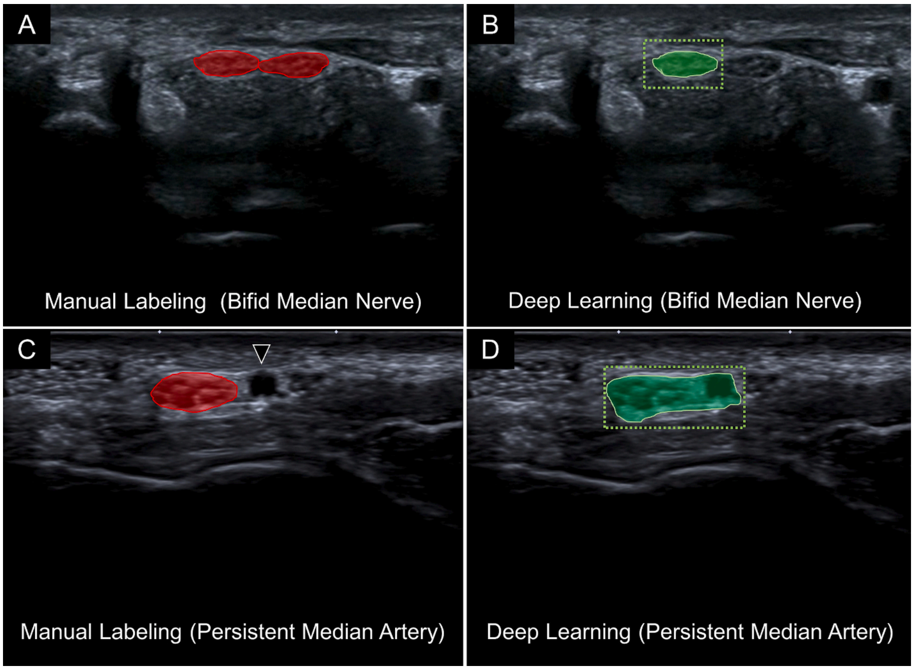

Fig. 6. The bifid median nerve is manually labelled by an expert (A). Only one portion of the bifid nerve is recognized by the deep learning algorithm (B). A persistent median artery (black arrowhead) is located beside the median nerve marked by an expert (C). The persistent median artery is misrecognized and included as part of the median nerve by the deep learning algorithm (D).
Red circle region, the ground truth of the median nerve; green square area, the predicted boundary box containing the median nerve; green circled area, the result of segmentation for the median nerve. (For interpretation of the references to colour in this figure legend, the reader is referred to the web version of this article.)

diagnosis [3,4]. Likewise, through our review, we identified different approaches for segmenting the median nerve. Hafiane et al. [23] used a CNN to first localize the median nerve and then segment it using a phase-based probabilistic active contour [31], whose feasibility was first examined using ultrasound imaging of the sciatic nerve. U-Net and Mask R-CNN emerged as the mainstream methods for nerve segmentation in later studies (Fig. 5) [24,27–29]. U-Net [15], with a symmetric U-shaped structure, is capable of restoring the extracted feature map to its input size by concatenating the convolution and transposed convolution layers. This counteracts the gradual loss of feature resolution when the framework deepens. On the other hand, Mask R-CNN [15] is a powerful model for instance segmentation, i.e., detecting the object's class and predicting its boundary box. It also incorporates an FPN [32], facilitating feature extraction on various scales. In our meta-analysis, the summarized Dice coefficient from five studies [23,24,26,27,29] reached 0.898, and the highest IOU from one study [28] was approximately 0.8216. All findings supported the application of deep learning algorithm for segmenting the median nerve on ultrasound imaging.

The strength of ultrasound imaging is its dynamic scanning capability. The transducer can be moved back and forth to track the median nerve and examine its continuity [33]. In our review, we noticed that Hafiane et al. [23] adjusted the movement of the transducer to capture different views of the median nerve in videos. Strictly speaking, this might not be categorized as dynamic imaging because there was little change in the location of the footprint. It is worth emphasizing that the median nerve in the distal forearm appears similar to the adjacent finger flexor tendons [33]; therefore, nerve localization could prove challenging for the deep learning algorithm. However, although the performance metrics for nerve localization seemed satisfactory in the study by Hafiane et al., [23] whether the outcome can be transferred to real-time dynamic tracking of the median nerve along the entire upper limb should be validated in future research.

On the other hand, Wu et al. [28] obtained dynamic images of the median nerve by inviting the participants to repetitively flex and extend their fingers. Facilitated by a deep learning algorithm, they identified that the cross-sectional area and perimeter of the median nerve increased during finger flexion and decreased upon finger extension. Disproportionation of the centroid displacement of the nerve on the horizontal and vertical axes was also observed. Their study demonstrated the usefulness of automated segmentation in continuously extracting the motion metrics of the median nerve during finger movements, which could be beneficial in determining whether abnormal nerve excursion exists owing to adhesion [34].

Anatomic variants such as persistent median arteries and bifid median nerves are commonly encountered during ultrasound imaging of the wrist region. According to an antecedent study investigating 1026 wrists of 513 manual laborers, the prevalence of bifid median nerve was approximately 8.6 % [35]. In patients with bifid median nerves, the diagnosis of CTS based on ultrasound images requires the additional measurement of the cross-sectional area of the nerve from different compartments [36]. This would definitely increase the difficulty in correctly recognizing the separate nerve parts with deep learning algorithms. Our meta-analysis revealed that Smerilli et al. [29] specifically addressed the aforementioned issue and found that the accuracy rate of nerve localization improved from 83.7 % to 95.3 % after removing the cases with anatomic variants. They also found that the deep learning algorithm might only classify one compartment or misrecognize the adjacent persistent median artery as the second nerve part (Fig. 6). Considering that a bifid median nerve has an increased association with CTS [36], future deep learning algorithms might need a difference layer to recognize the existence of normal anatomic variants before proceeding to subsequent nerve localization and segmentation.

This systematic review and meta-analysis has several limitations. First, regarding manual labelling of the nerve circumference, none of the included studies provided details of whether the boundary lines were drawn on the epineurium or outside the epineurium of the median nerve. The most commonly used criterion for diagnosing CTS is based on the cross-sectional area of the nerve inside the epineurium [37]. Therefore, we believe that it would be more clinically relevant if future investigators could elaborate on how they perform hand-operated segmentation. Second, the majority of the enrolled studies used only one ultrasound imaging system for the median nerve. It is known that the same nerve would have distinct sonographic presentations with different settings/machines. The model trained by the images obtained from one system may show different performance metrics based on the data of another system. Therefore, future studies are warranted to validate the performance of deep learning algorithms across imaging datasets derived from various ultrasound manufacturers. Third, through our systematic review, we found that simultaneous identification of the anatomic landmarks adjacent to the median nerve was hardly achieved by using conventional deep learning algorithms. Multi-scale deep learning algorithms that integrate information at the receptive fields of various scales could be employed to overcome the aforementioned drawbacks in the future [38,39]. Furthermore, a manually defined ROI was usually needed in advance for some early deep learning models for nerve localization and segmentation. This process appeared time-consuming and was dependent on the reliability of labelling experts. Recently, a fully automatic Mask R-CNN, trained by an end-to-end approach without needing the definition of ROI, has been developed and it would be helpful to compensate the above quoted shortcoming [40].

5. Conclusion

The deep learning algorithm enables automatic localization and segmentation of the median nerve at the wrist on ultrasound imaging with acceptable accuracy and precision. The motion metrics of the median nerve under dynamic ultrasound imaging can be automatically extracted using a deep-learning algorithm. It is recommended that future researches validate the performance of deep learning algorithms in the detection and segmentation of the median nerve along its entire length as well as across datasets obtained from various ultrasound manufacturers.

Funding/support

K.V·C received funding from (1) National Taiwan University Hospital, Bei-Hu Branch; (2) Ministry of Science and Technology (MOST 106–2314-B-002–180-MY3 and 109–2314-B-002–114-MY3); (3) Taiwan Society of Ultrasound in Medicine.

Declaration of competing interest

Each author certifies that he or she has no commercial associations.

Appendix A. Supplementary data

Supplementary data to this article can be found online at https://doi.org/10.1016/j.artmed.2023.102496.

References

[1] Burton CL, Chen Y, Chesterton LS, van der Windt DA. Trends in the prevalence, incidence and surgical management of carpal tunnel syndrome between 1993 and 2013: an observational analysis of UK primary care records. BMJ Open 2018;8(6):e020166.
[2] Stevens JC. AAEM minimonograph #26: the electrodiagnosis of carpal tunnel syndrome. American Association of Electrodiagnostic Medicine. Muscle Nerve 1997;20(12):1477–86.
[3] Torres-Costoso A, Martínez-Vizcaíno V, Álvarez-Bueno C, Ferri-Morales A, Cavero-Redondo I. Accuracy of ultrasonography for the diagnosis of carpal tunnel syndrome: a systematic review and meta-analysis. Arch Phys Med Rehabil 2018;99(4):758–65. e10.
[4] Tai TW, Wu CY, Su FC, Chern TC, Jou IM. Ultrasonography for diagnosing carpal tunnel syndrome: a meta-analysis of diagnostic test accuracy. Ultrasound Med Biol 2012;38(7):1121–8.
[5] Lin CP, Chen IJ, Chang KV, Wu WT, Özçakar L. Utility of ultrasound elastography in evaluation of carpal tunnel syndrome: a systematic review and meta-analysis. Ultrasound Med Biol 2019;45(11):2855–65.
[6] Evans KD, Roll SC, Volz KR, Freimer M. Relationship between intraneural vascular flow measured with sonography and carpal tunnel syndrome diagnosis based on electrodiagnostic testing. J Ultrasound Med 2012;31(5):729–36.
[7] Lo IN, Hsu PC, Huang YC, Yeh CK, Yang YC, Wang JC. Dynamic ultrasound assessment of median nerve mobility changes following corticosteroid injection and carpal tunnel release in patients with carpal tunnel syndrome. Front Neurol. 2021;12:710511.
[8] Chen IJ, Chang KV, Lou YM, Wu WT, Özçakar L. Can ultrasound imaging be used for the diagnosis of carpal tunnel syndrome in diabetic patients? A systemic review and network meta-analysis. J Neurol 2020;267(7):1887–95.
[9] Hadjerci O, Hafiane A, Conte D, Makris P, Vieyres P, Delbos A. Computer-aided detection system for nerve identification using ultrasound images: a comparative study. Informatics Med Unlocked 2016;3:29–43.
[10] Kim M, Yan C, Yang D, Wang Q, Ma J, Wu G. Chapter eight - deep learning in biomedical image analysis. In: Feng DD, editor. Biomedical information technology. (Second Edition). Academic Press; 2020. p. 239–63.
[11] Yamashita R, Nishio M, Do RKG, Togashi K. Convolutional neural networks: an overview and application in radiology. Insights Imaging 2018;9(4):611–29.
[12] Smistad E, Johansen KF, Iversen DH, Reinertsen I. Highlighting nerves and blood vessels for ultrasound-guided axillary nerve block procedures using neural networks. J Med Imaging (Bellingham) 2018;5(4):044004.
[13] Huang C, Zhou Y, Tan W, et al. Applying deep learning in recognizing the femoral nerve block region on ultrasound images. Ann Transl Medicine 2019;7(18):453.
[14] Whiting PF, Rutjes AW, Westwood ME, et al. QUADAS-2: a revised tool for the quality assessment of diagnostic accuracy studies. Ann Intern Med 2011;155(8):529–36.
[15] Malhotra P, Gupta S, Koundal D, Zaguia A, Enbeyle W. Deep neural networks for medical image segmentation. J Healthcare Eng 2022;2022:9580991.
[16] Riley RD, Higgins JP, Deeks JJ. Interpretation of random effects meta-analyses. BMJ 2011;342:d549.
[17] Higgins JPT, Thompson SG, Deeks JJ, Altman DG. Measuring inconsistency in meta-analyses. BMJ 2003;327(7414):557–60.
[18] Lin L, Chu H. Quantifying publication bias in meta-analysis. Biometrics 2018;74(3):785–94.
[19] Hadjerci O, Hafiane A, Morette N, Novales C, Vieyres P, Delbos A. Assistive system based on nerve detection and needle navigation in ultrasound images for regional anesthesia. Expert Syst Appl 2016;61:64–77.
[20] Alkhatib M, Hafiane A, Tahri O, Vieyres P, Delbos A. Adaptive median binary patterns for fully automatic nerves tracking in ultrasound images. Comput Methods Programs Biomed 2018;160:129–40.
[21] Kakade A, Dumbali J. Identification of nerve in ultrasound images using U-net architecture. In: International conference on communication information and computing technology (ICCICT); 2018.
[22] Wong AL, Hricz N, Malapati H, et al. A simple and robust method for automating analysis of naïve and regenerating peripheral nerves. PLoS One 2021;16(7):e0248323.
[23] Hafiane A, Vieyres P, Delbos A. Deep learning with spatiotemporal consistency for nerve segmentation in ultrasound images. ArXiv 2017. abs/1706.05870.
[24] Horng MH, Yang CW, Sun YN, Yang TH. DeepNerve: a new convolutional neural network for the localization and segmentation of the median nerve in ultrasound image sequences. Ultrasound Med Biol 2020;46(9):2439–52.
[25] Wang YW, Chang RF, Horng YS, Chen CJ. MNT-DeepSL: median nerve tracking from carpal tunnel ultrasound images with deep similarity learning and analysis on continuous wrist motions. Comput Med Imaging Graph 2020;80:101687.
[26] Cosmo MD, Chiara Fiorentino M, Villani FP, et al. Learning-based median nerve segmentation from ultrasound images for carpal tunnel syndrome evaluation. Annu Int Conf IEEE Eng Med Biol Soc 2021;2021:3025–8.
[27] Festen RT, Schrier V, Amadio PC. Automated segmentation of the median nerve in the carpal tunnel using U-net. Ultrasound Med Biol 2021;47(7):1964–9.
[28] Wu CH, Syu WT, Lin MT, et al. Automated segmentation of median nerve in dynamic sonography using deep learning: evaluation of model performance. Diagnostics (Basel) 2021;11(10):1893.
[29] Smerilli G, Cipolletta E, Sartini G, et al. Development of a convolutional neural network for the identification and the measurement of the median nerve on ultrasound images acquired at carpal tunnel level. Arthritis Res Ther 2022;24(1):38.
[30] Zhang R, Du L, Xiao Q, Liu J. Comparison of backbones for semantic segmentation network. J Phys Conf Ser 2020;1544(1):012196.
[31] Hafiane A, Vieyres P, Delbos A. Phase-based probabilistic active contour for nerve detection in ultrasound images for regional anesthesia. Comput Biol Med 2014;52:88–95.
[32] Yu G, Wu Y, Xiao J, Cao Y. A novel pyramid network with feature fusion and disentanglement for object detection. Comput Intell Neurosci 2021;2021:6685954.
[33] Wu CH, Chang KV, Özçakar L, et al. Sonographic tracking of the upper limb peripheral nerves: a pictorial essay and video demonstration. Am J Phys Med Rehabil 2015;94(9):740–7.
[34] Chang KV, Wu WT, Özçakar L. Ultrasound imaging and guidance in peripheral nerve entrapment: hydrodissection highlighted. Pain Manag 2020;10(2):97–106.
[35] Walker FO, Cartwright MS, Blocker JN, et al. Prevalence of bifid median nerves and persistent median arteries and their association with carpal tunnel syndrome in a sample of Latino poultry processors and other manual workers. Muscle Nerve 2013;48(4):539–44.
[36] Klauser AS, Halpern EJ, Faschingbauer R, et al. Bifid median nerve in carpal tunnel syndrome: assessment with US cross-sectional area measurement. Radiology 2011;259(3):808–15.
[37] Wu WT, Chen LR, Chang HC, Chang KV, Özçakar L. Quantitative ultrasonographic analysis of changes of the suprascapular nerve in the aging population with shoulder pain. Front Bioeng Biotechnol 2021;9:640747.
[38] Ding Y, Yang Q, Wu G, Zhang J, Qin Z. Multiple Instance Segmentation in Brachial Plexus Ultrasound Image Using BPMSegNet. ArXiv; 2020. abs/2012.12012.
[39] Kim BS, Yu M, Kim S, Yoon JS, Baek S. Scale-attentional U-net for the segmentation of the median nerve in ultrasound images. Ultrasonography 2022;41(4):706–17.
[40] Al-Battal AF, Gong Y, Xu L, et al. A CNN segmentation-based approach to object detection and tracking in ultrasound scans with application to the vagus nerve detection. Annu Int Conf IEEE Eng Med Biol Soc 2021;2021:3322–7.